Life Sciences 219 (2019) 353–363

Contents lists available at ScienceDirect

Life Sciences

journal homepage: www.elsevier.com/locate/lifescie

Transcription profiling of artemisinin-treated diabetic nephropathy rats using high-throughput sequencing

Min Xiang, Zhihong Chen, Liangping He, Guoliang Xiong, Jiandong Lu*

Department of Nephrology, Shenzhen Traditional Chinese Medicine Hospital, The Fourth Clinical Medical College of Guangzhou University of Chinese Medicine, Shenzhen 518033, Guangdong, China

ARTICLE INFO

Keywords:
Diabetic nephropathy
Artemisinin
RNA-sequencing

ABSTRACT

Artemisinin (Art) plays a renoprotective role in diabetic nephropathy (DN) rats. However, the differential gene expression profile and underlying molecular mechanism of Art treatment in DN is not well understood. We constructed an animal model of DN by injection of streptozotocin (STZ) in rats. We then examined the profile of differentially expressed genes following administration of Art using RNA-sequencing (KANGCH&EN, Shanghai, China). Five genes identified by RNA-sequencing were randomly selected and validated by qRT-PCR. Bioinformatic analyses were performed to study these differentially expressed genes. We identified a total of 31 genes that were significantly up-regulated in DN samples compared to both normal and Art treatment samples, and 38 genes that were significantly down-regulated in DN samples compared to both normal and Art treatment samples. The identified genes were associated with a list of gene ontology (GO) terms and Kyoto Encyclopedia of Genes and Genomes (KEGG) pathways and may be involved in the mechanism underlying Art treatment of DN. Thus, the results from the current study demonstrate that genes are aberrantly expressed after Art treatment and identify promising targets in the treatment of DN with artemisinin.

1. Introduction

Diabetic nephropathy (DN) is a serious complication of diabetes [1,2]. It is the main cause of death and disability in diabetes patients. Delays in the diagnosis and treatment of DN may leave dialysis and kidney transplantation as the only treatment options, especially during later stages of renal disease [3–5]. The early pathological features of DN are glomerular hypertrophy, thickening of glomerular and renal tubule basement membranes, and accumulation of extracellular matrix in the mesangial region, while the later pathological features of DN are glomerular and renal tubulointerstitial fibrosis [6,7]. Early clinical manifestations of DN include reduction in glomerular filtration, followed by elevated arterial blood pressure, proteinuria and fluid retention, and eventually renal failure [2,4,8]. However, the pathogenesis of DN is complex and is not fully understood yet.

Artemisinin (Art) and its derivatives have become widely recognized as preferred antimalarial drugs worldwide [9,10]. Semisynthetic derivatives of artemisinin have been developed, including artesunate (water-soluble: for oral, rectal, intramuscular, or intravenous use), artemether (lipid-soluble: for oral, rectal or intramuscular use), dihydroartemisinin, artelinic acid, artemotil shows great promising in the treatment of malaria. In addition to its antimalarial effects, Art and its derivatives were found to have pharmacological effects in other areas, including anti-tumor [11,12], immune suppressive [13,14], anti-fibrosis [15], anti-obesity [16], anti-fungal, and anti-diabetes [17] effects. Recently, Kubicek and colleagues investigated the effects of a representative library of approved drugs on cultured alpha cells and found that Art changes the epigenetic program of glucagon-producing alpha cells and induces profound alterations in their biochemical function [18]. The Kubicek team also made the breakthrough discovery that Art was able to convert glucagon-producing alpha cells into insulin-producing beta cells. Zhang et al. investigated the role of Art in the expression of protein kinase C PKC, platelet-derived growth factor PDGFB, matrix metallopeptidase MMP2, and tissue inhibitor of metalloproteinase TIMP2 in diabetic rats [19–21]. They found that treatment with Art partially reversed the increases in protein expression of PKC, PDGFB, fibronectin, collagen IV, and TIMP2 in glomeruli, and also partly reversed the decrease in MMP2 protein levels. Zhou et al. found that Art significantly suppressed the DNA-binding activity of activator protein 1 and the DNA-binding activity of nuclear factor kappa light chain enhancer of activated B cells (NF-κB), reversed the increases in expression of c-fos and c-jun in kidney of rats, and alleviated renal

* Corresponding author at: Department of Nephrology, Shenzhen Traditional Chinese Medicine Hospital, The Fourth Clinical Medical College of Guangzhou University of Chinese Medicine, No. 1 Fuhua Road, Shenzhen 518033, Guangdong, China.
E-mail address: lujiandong@yeah.net (J. Lu).

https://doi.org/10.1016/j.lfs.2019.01.032
Received 13 November 2018; Received in revised form 18 January 2019; Accepted 18 January 2019
Available online 23 January 2019

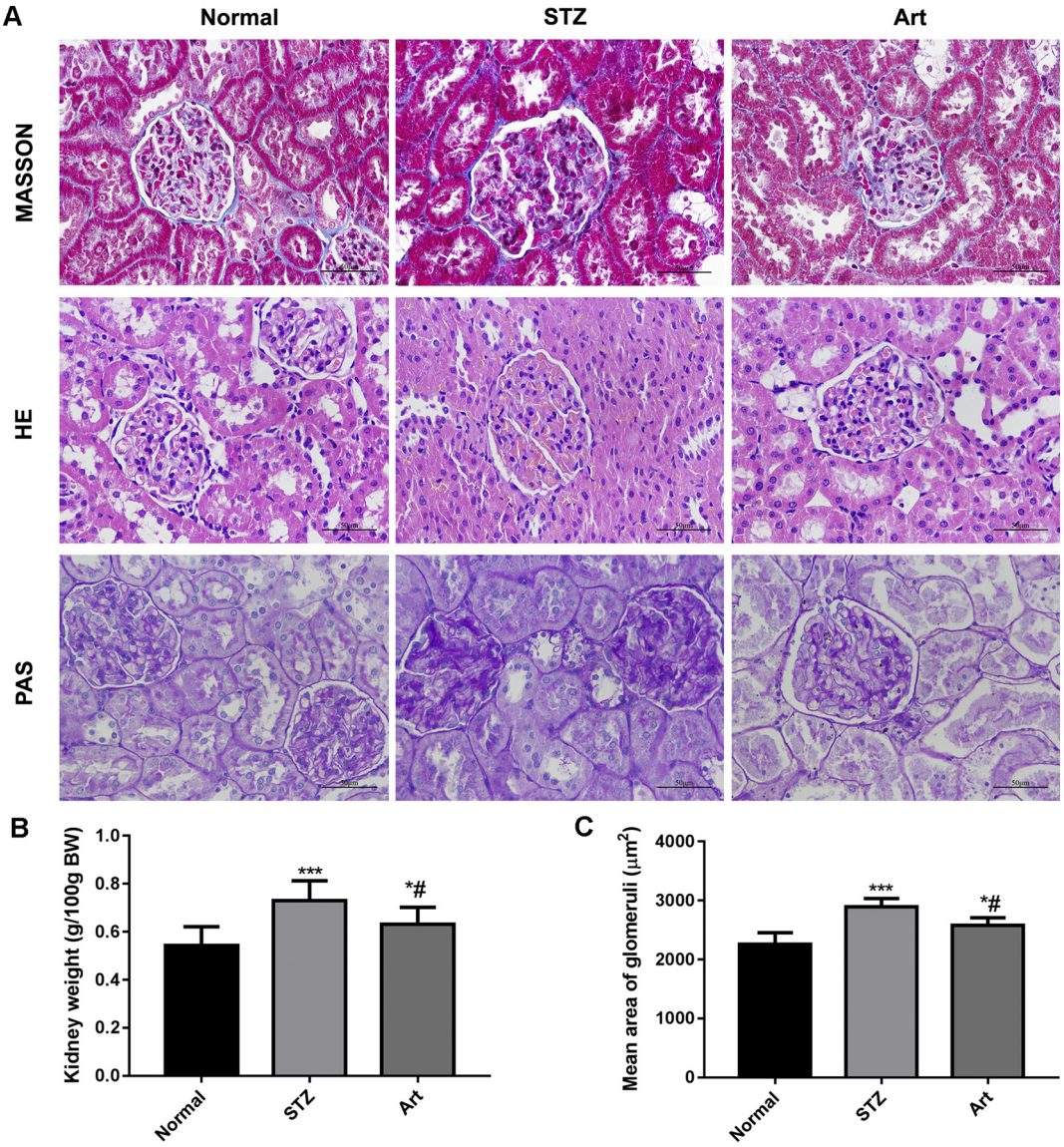

Fig. 1. Pathologic analysis of DN samples with Art treatment. DN model was induced by STZ, and treated with artemisinin Art. (A) Representative Masson staining images, hematoxylin and eosin staining images and PAS staining images. Magnification, 400×. (B) Relative kidney weight. (C) The mean area of glomeruli. $^{*}P < 0.05$, $^{***}P < 0.01$ vs. normal, $\#P < 0.05$ vs. Art.

pathological changes in diabetic rats [22–24]. Thus, Art has renoprotective effects in diabetic rats. However, less is known about the mechanism underlying Art treatment of DN, and genomic sequencing following Art treatment has not been reported. The use of next-generation sequencing for ditag genome scanning (DGS) has increased considerably [25]. Brennan et al. identified a shared subset of 179 regulated genes in RNA-Seq using microarray, including several genes not previously available in microarray platforms. Of note, *Ark5*, encoding an AMP-related kinase, and *Tgfbi*, encoding transforming growth factor, beta-induced protein were induced by TGF-beta1 and also upregulated in human DN. It was thus proposed that TGF-beta1-driven pro-fibrotic signal may play a critical role in renal epithelial cells through the analysis of DN renal transcriptome [26]. Using high-throughput RNA-Seq, a set of inflammatory gene pathways was identified from among hundreds of differentially expressed genes; the identified pathways revealed potential pathogenic mechanisms in progressive chronic kidney disease in DN rats [27]. The present study was conducted to investigate the mechanism of Art treatment of DN. In this study, a new generation sequencing technology platform, Illumined genome analyzer IIx, was used to investigate the entire transcriptome and mechanism of Art-treated DN.

2. Material and methods

2.1. Animals and experimental design

This study was approved by the Ethics Committee of the Guangzhou University of Chinese Medicine (Guangzhou, China), and all experiments were performed in accordance with the National Institutes of Health Guide for the Care and Use of Laboratory Animals. Male Sprague-Dawley (SD) rats (n = 18; weight 250–300 g) were purchased from the experimental animal center of Guangzhou University of Chinese Medicine and were maintained for 1 week in an environment with controlled humidity (55 ± 15%), temperature (23 ± 3 °C), and a 12-h light-dark cycle. All rats had a mean ± standard deviation fasting blood glucose (FBG) of 6.2 ± 1.7 mmol/L. Rats were randomly divided into three groups: normal control (n = 6, equal volume of saline; control), STZ administration model group (n = 6, equal volume of saline; STZ), and the STZ administration and Art treatment group (n = 6, 300 mg/kg/d; Art, oral gavage) according to previous study [28].

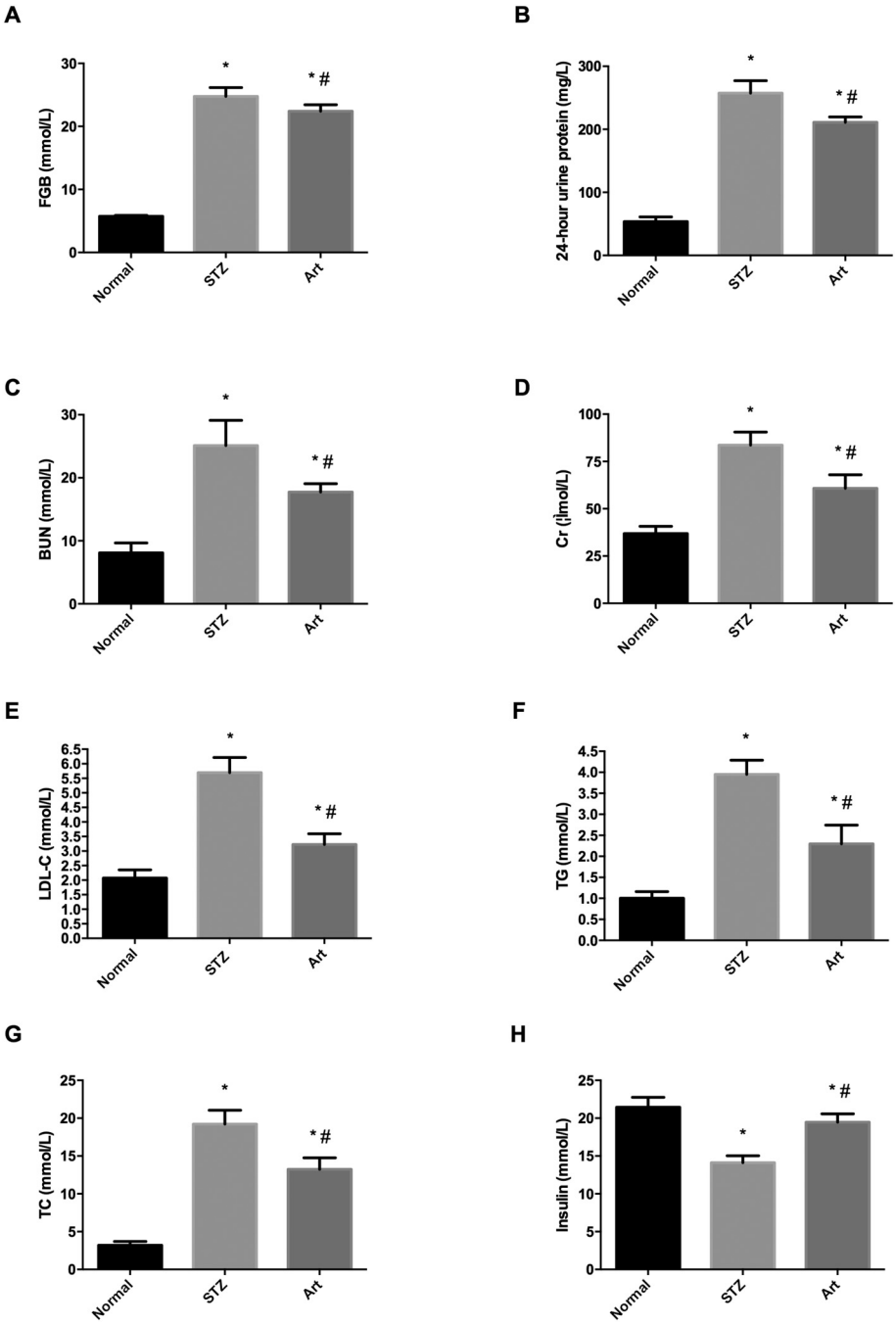

Fig. 2. Biochemical indices. (A) Fasting blood glucose (FBG). (B) Urine protein. (C) Blood urea nitrogen (BUN). (D) Creatinine (Cr). (E) Low density lipoprotein cholesterol (LDL-C). (F) Triglyceride (TG). (G) Total cholesterol (TC). (H) Insulin. *$P < 0.05$ vs. normal. #$P < 0.05$ vs. STZ.

Particularly, as previously described [29], the rats in the STZ group were injected intraperitoneally with 60 mg/kg STZ (prepared with 0.1 mol/L citrate buffer, pH 4.5) once. After 72 h, fasting blood glucose (FBG) and urine volume were measured, and urine protein level was detected using Bradford method. If the following criteria were met three times in succession, the DN model was considered to be established: (1) FBG > 16.6 mmol/L; (2) urine volume > 150% of the original volume; (3) 24 h urinary protein > 200% before modeling. Once the DN model was established, Art (300 mg/kg/d) was administered for the next 4 weeks. The rats were then anesthetized with chloral hydrate. After abdominal aorta was washed with phosphate-buffered saline (PBS), the kidneys were cut from 1 mm away from the renal lobe and stored in −80 °C for later examination.

2.2. Masson, hematoxylin and eosin (H&E), and periodic acid–Schiff (PAS) staining techniques

The kidneys were fixed in 4% paraformaldehyde. To confirm the STZ model and Art treatment, Masson, H&E, and PAS staining techniques were performed as previously described [30,31].

2.3. Biochemical indexes

In order to confirm the construction of the model, urine samples were collected from rats 24 h before they were sacrificed, and the level of urinary albumin was measured. The rats were fasted for 12 h and then anesthetized by intraperitoneal injection with 40 mg/kg of a solution of 2% sodium pentobarbital in saline. Blood was collected from

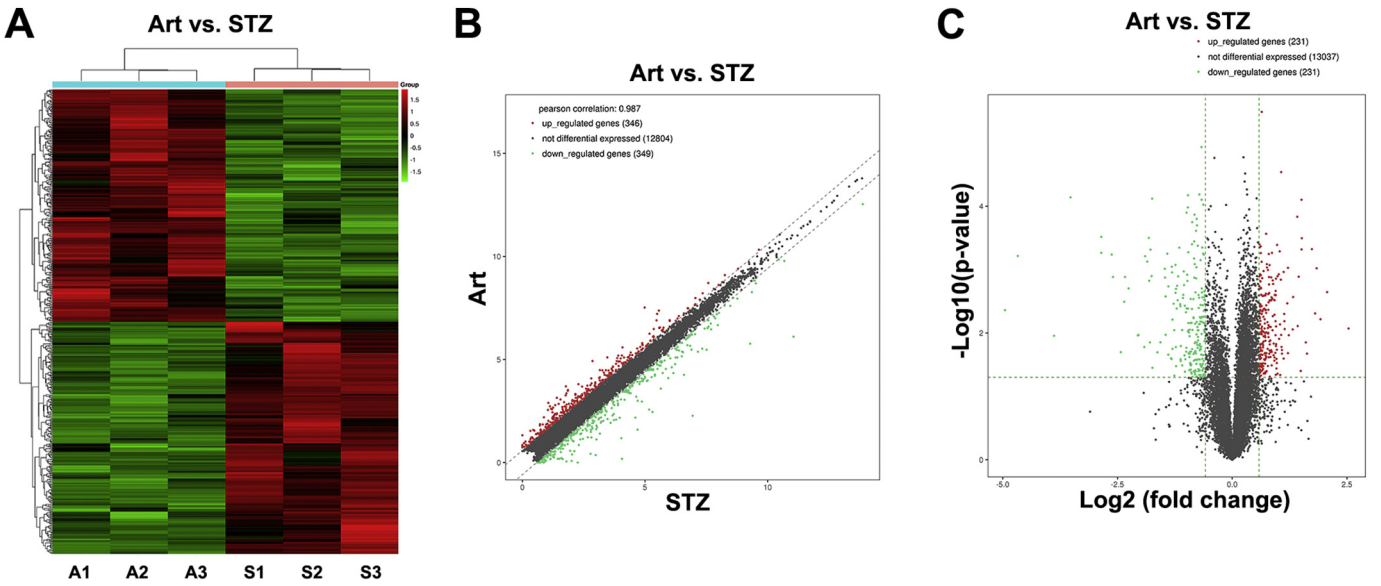

Fig. 3. Overview of RNA-Seq data. (A) Hierarchical clustering of gene expression data based on FPKM values between Art (A) and STZ (S) samples. (B) Scatter plot showing the gene expression variation between Art (A) and STZ (S) samples. The red and green points indicated change greater than and < 2-fold for genes between the two groups. (C) Volcano plot of the differentially expressed genes. The vertical lines correspond to 2-fold up and down, respectively, and the horizontal line indicates *P* value 0.05. The red and green points in the plots represent the significantly up-regulated and down-regulated differentially expressed genes. (For interpretation of the references to color in this figure legend, the reader is referred to the web version of this article.)

Table 1
Genes significantly up-regulated in STZ samples compared to either normal samples or Art samples.

Gene name	FPKM								
	Normal1	Normal2	Normal3	Art1	Art2	Art3	STZ1	STZ2	STZ3
Slco1a1	3.32	7.85	1.93	33.97	64.35	46.03	194.26	156.37	144.63
Cyp2c11	55.12	20.06	25.23	14.70	20.90	32.51	60.04	84.67	77.68
Tff3	52.04	56.57	51.80	168.97	241.44	323.17	800.23	645.38	717.22
Rgd1564999	1.37	1.67	0.85	8.72	7.12	8.87	44.23	25.67	33.29
Gc	3.21	6.46	4.22	15.81	24.08	16.64	29.34	43.62	50.38
Tm4sf20	0.47	0.33	0.09	4.79	3.25	6.34	9.64	10.83	12.37
Slc7a12	6.72	4.76	3.72	15.39	38.10	25.97	46.85	35.28	57.04
Cacng5	1.08	6.89	4.69	26.52	10.03	11.26	75.46	40.55	30.12
Aldh1b1	0.47	0.52	0.09	2.99	2.62	2.54	12.23	8.09	7.53
Gtpbp4	20.18	20.09	14.52	47.27	39.38	75.36	206.94	152.34	97.66
Rgn	40.21	28.79	69.93	56.07	119.66	102.18	337.16	200.29	234.31
Melk	0.98	1.29	1.26	3.55	6.39	2.81	10.47	15.32	10.28
Ptgds	18.23	16.28	14.09	30.62	15.72	39.96	94.36	66.51	73.64
Slc16a14	17.46	18.16	22.52	39.59	36.43	30.61	109.21	85.76	93.45
Hnmt	49.00	51.84	35.92	82.61	106.34	96.26	221.53	194.67	285.19
Car15	2.09	3.82	5.18	10.96	8.16	5.30	38.26	27.71	36.95
Dio1	36.25	49.39	37.22	52.76	60.99	95.66	134.65	185.48	196.51
Kifc1	1.32	2.52	1.28	6.95	8.89	12.26	23.56	18.09	17.84
Spata22	2.84	6.65	1.58	5.90	6.80	6.85	15.27	26.16	14.48
Anxa13	0.30	0.40	0.25	4.25	5.48	7.24	10.24	8.76	15.43
Slc25a25	20.67	21.78	29.20	43.81	44.16	37.69	83.46	92.17	90.35
Slc22a22	21.08	26.13	33.25	46.08	42.78	33.01	105.84	112.57	86.33
Nefm	0.45	0.59	1.54	2.69	1.90	2.90	5.63	7.22	9.95
Prlr	6.85	10.03	7.85	25.04	14.75	19.78	43.28	30.47	51.08
Cxcl13	1.76	1.87	2.61	2.89	5.78	3.04	12.45	13.11	9.84
Gas2	4.68	3.59	3.42	5.68	8.15	10.05	25.48	18.23	25.01
Mmp9	7.14	14.03	13.24	5.39	10.30	3.54	10.22	19.06	15.17
Hmgcs2	10.68	16.47	11.97	16.70	11.53	6.57	43.85	65.87	50.21
Id1	43.52	35.01	36.93	33.50	34.55	54.74	83.04	113.58	94.77
Cdkn1a	26.17	33.61	28.73	22.68	31.74	2.20	94.57	189.76	134.51
Rarres2	63.90	34.85	49.85	40.27	63.84	44.52	121.44	194.28	109.19

tail vein. FBG was measured by Accu-check active (Roche, Shanghai, China). Urine protein, blood urea nitrogen (BUN), serum cholesterol (TC), triglyceride (TG), creatinine (Cr), low density lipoprotein cholesterol (LDL-C) insulin were detected by an automatic biochemical analyzer (ADVIA1800, Siemens, Munich, Germany). Statistical analysis was performed using the Student's *t*-test in the SPSS version 16.0 software (SPSS, USA). A *P* value < 0.05 was considered significant.

2.4. RNA extraction and quality control

The kidney was harvested for mRNA enrichment. In brief, total RNA was extracted from samples using Trizol (Invitrogen, USA) according to

Table 2
Genes significantly down-regulated in STZ samples compared to either normal samples or Art samples.

Gene name	FPKM								
	Normal1	Normal2	Normal3	Art1	Art2	Art3	STZ1	STZ2	STZ3
Igfbp1	225.15	264.92	101.30	171.98	133.78	145.77	47.26	30.18	34.67
Fst	10.88	11.51	13.63	3.85	6.16	15.48	1.73	2.53	1.86
Fibin	7.88	5.46	6.18	4.32	5.28	3.80	1.04	0.98	1.24
Sult1a1	182.54	136.36	178.59	21.64	33.99	44.75	10.03	13.25	15.56
Defb28	9.21	8.20	6.30	1.82	4.72	5.15	0.94	1.12	1.23
Ddit4l	5.70	14.37	12.52	1.72	2.32	3.11	0.75	1.03	1.26
Inhbb	3.67	8.14	5.82	4.35	3.40	4.63	1.32	1.57	0.93
Lox	4.98	5.19	4.44	2.52	3.42	1.02	1.35	0.87	1.10
Fgb	5.06	5.84	6.92	3.05	2.10	2.58	1.45	1.22	0.81
Pigr	128.54	124.46	103.23	86.58	63.99	70.77	44.32	23.58	35.54
Cldn23	4.53	5.79	5.82	4.60	2.72	7.40	1.86	1.07	2.29
Steap4	24.73	20.18	19.66	16.84	14.30	13.77	10.83	7.61	6.38
Lcn2	5.67	7.88	6.49	4.31	4.81	2.10	2.61	1.95	0.81
Csdc2	3.90	6.98	3.08	2.07	2.08	1.63	0.57	0.84	1.11
Gpt	24.99	18.07	21.20	16.38	14.37	11.18	7.18	6.24	5.39
Gsta3	30.42	30.35	37.22	18.68	19.04	15.65	10.23	6.52	7.64
Baat	30.86	46.25	31.49	21.97	16.56	25.10	10.05	9.37	8.18
Spp1	434.31	363.53	463.86	251.42	337.96	380.61	185.64	146.31	176.83
Rnase4	10.32	8.61	7.41	6.37	7.08	8.06	2.73	3.58	1.94
Resp18	77.89	99.47	88.38	56.28	76.64	60.11	33.15	38.62	30.37
Slc22a7	15.16	13.05	9.32	9.96	8.45	7.66	1.23	5.34	3.65
Pdk4	21.75	15.31	28.86	14.06	15.20	13.77	7.56	6.39	5.12
Arg2	77.82	71.26	76.26	47.38	47.32	60.28	23.56	17.08	29.87
Fzd9	2.09	1.48	2.25	0.21	0.38	1.22	0.12	0.15	0.29
Apoc2	32.19	21.26	48.31	20.43	12.52	18.94	10.38	6.73	9.62
Tnfsf15	3.73	4.73	3.88	2.66	3.47	2.80	1.22	1.08	1.45
Gadd45b	13.70	14.19	6.73	7.07	8.83	8.12	3.35	2.41	3.88
Bcl2l11	4.07	3.41	3.61	3.78	2.46	2.24	1.53	0.98	1.27
Nupr1l1	35.76	34.71	29.49	24.60	24.01	40.07	11.64	10.55	21.36
Stc1	33.99	24.89	22.33	19.68	21.00	25.13	10.37	11.82	7.24
Fga	26.95	31.99	16.36	15.42	16.65	22.28	5.76	8.19	9.63
Tp53inp1	21.80	19.06	22.66	16.74	14.74	18.44	7.63	5.05	9.39
Pmaip1	5.74	5.15	4.26	3.49	4.12	5.32	2.01	1.43	0.99
Cebpd	20.80	34.68	19.08	25.77	13.21	13.02	11.82	5.38	6.42
Rnf125	6.85	8.23	5.84	4.81	4.33	5.16	2.13	1.65	2.44
Unc93a	5.13	6.25	7.29	4.75	3.04	3.95	2.06	1.73	1.58
Cyp26b1	3.83	4.77	3.62	2.03	3.41	2.60	0.92	1.36	1.05
Vnn1	93.65	85.60	94.45	70.37	65.08	75.90	35.29	29.76	36.51

the manufacturer's protocol and was subjected to 1% agarose gel electrophoresis and Nanodrop ND-1000 (NanoDrop, USA) for quality and purity tests, respectively. The ratios of OD260/OD280 in all samples were between 1.8 and 2.0, indicating high purity of the extracted RNA. Pollutants such as protein and phenols were absent. The OD260/OD230 ratios in all samples were > 2, indicating an absence of organic extraction reagent contamination. The Q30 value of each sample was > 80%. Thus, the samples met quality and purity requirements for high-throughput sequencing.

2.5. mRNA sequencing

Kidney samples were sent to KANGCH&EN for RNA sequencing and analysis (Shanghai, China) as reported previously [32]. Oligo (dT) beads were used to enrich the mRNA after removal of rRNA using RiboZero Magnetic Gold Kit, Illumina, USA. The RNA sequencing library was created using the KAPA Stranded RNA-Seq Library Prep Kit (Illumina, USA), following the protocol provided by manufacturer. Quality control of the constructed library was performed using the Agilent 2100 Bioanalyzer (Agilent, Germany) and quantified by the qPCR method. Finally, the DNA fragments in these libraries were denatured by 0.1 mol/L NaOH to generate single-strand DNA, loaded onto channels of Illumina flow cell at a concentration of 8 pmol/L, amplified in situ using TruSeq SR Cluster Kit v3-cBot-HS (#GD-401-3001, Illumina), and subsequently sequenced for 150 cycles in the Illumina HiSeq 4000 according to the manufacturer's instructions.

2.6. Bioinformatics analysis

Image analysis and base calling were performed using Solexa pipeline version 1.8 (Off-Line Base Caller software, version 1.8) [33]. After quality testing using Fast QC software, trimmed reads were aligned to reference genomes using Hisat2 software version 2.0.4. Transcript abundance was estimated by using StringTie software version 1.2.3 and annotation information in the official database. Transcript levels were calculated as FRKM (fragments per kilobase cDNA per million fragments mapped) using Ballgown software [34]. Genes or transcripts with an FRKM > 0.5 were included in the subsequent analysis. Significant differentially expressed genes were identified as such if the fold change was larger than 2.0 and the *P*-value was < 0.05. Clustering analysis of differentially expressed genes was performed. Enriched gene ontology (GO) for annotated differentially expressed genes and Enriched KEGG (Kyoto Encyclopedia of Genes and Genomes) pathways were performed. A false discovery rate (FDR) < 0.05 was considered the threshold for significant enrichment.

2.7. Quantitative real time RT-PCR (qRT-PCR)

For validation of differentially expressed genes obtained in the transcriptome analysis, we detected the eight significant genes including inhibitor of DNA binding (*Id1*), insulin-like growth factor binding protein 1 gene (*Igfbp1*), cyclin dependent kinase inhibitor 1A (*Cdkn1a*), 3-hydroxy-3-methylglutaryl-CoA (HMG-CoA) synthase 2 (*Hmgcs2*), retinoic acid receptor responder 2 (*Rarres2*), Sulfotransferase

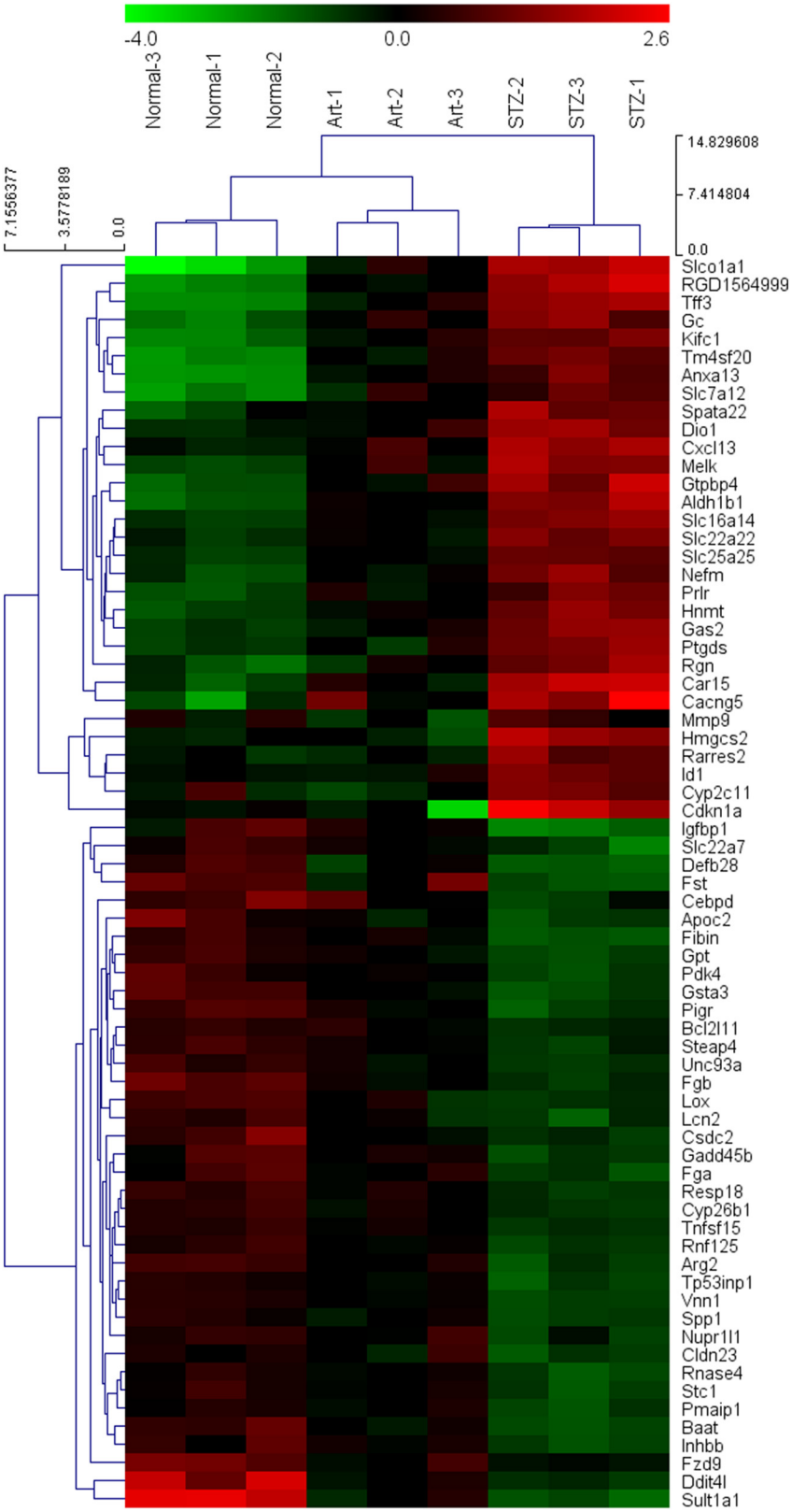

Fig. 4. Unsupervised hierarchical clustering of the 70 common differentially expressed genes between STZ/normal and STZ/Art groups. A total of 39 genes significantly were up-regulated in STZ samples compared to either normal samples or Art samples, and 31 genes were significantly down-regulated in STZ samples compared to either normal samples or Art samples. The unsupervised hierarchical clustering of the 70 common differentially expressed genes was performed to separate normal, Art, and STZ groups.

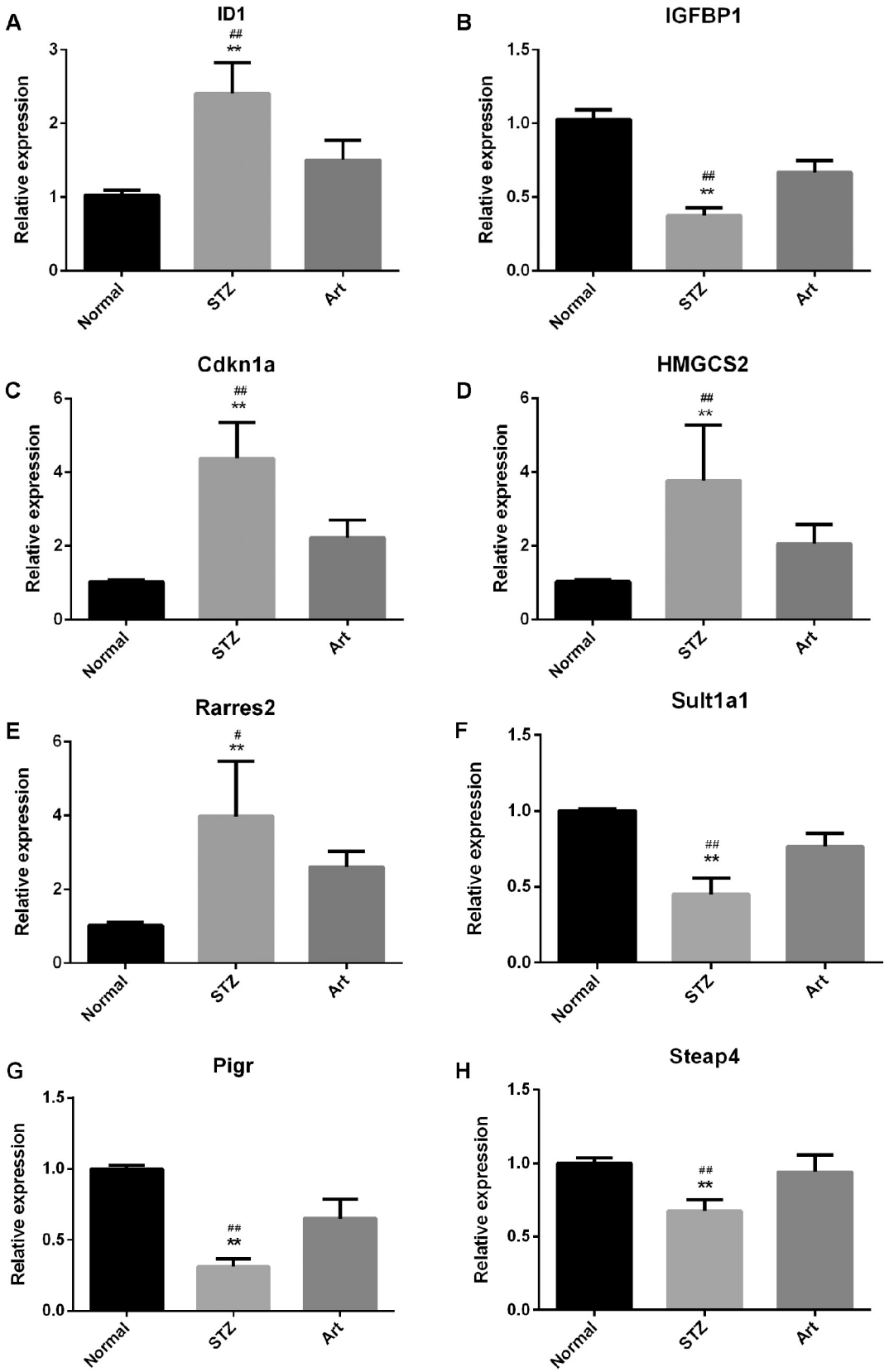

Fig. 5. Verification of differentially expressed genes. Five differentially expressed genes were randomly selected and the mRNA levels were measured by qRT-PCR. $^{**}P < 0.01$ vs. normal, $\#P < 0.05$, $\#\#P < 0.01$ vs. Art.

1A1 (*Sult1a1*), Polymeric immunoglobulin receptor (*Pigr*) and Six-transmembrane epithelial antigen of prostate4 (*Steap4*) by real-time PCR. Primers are described in Supplementary Table S1. RNA samples from the normal, STZ, and Art groups were extracted and purified, and cDNAs were synthesized using the PrimeScript™ RT Reagent Kit (TaKaRa, Japan) according to the manufacturer's protocol. PCR

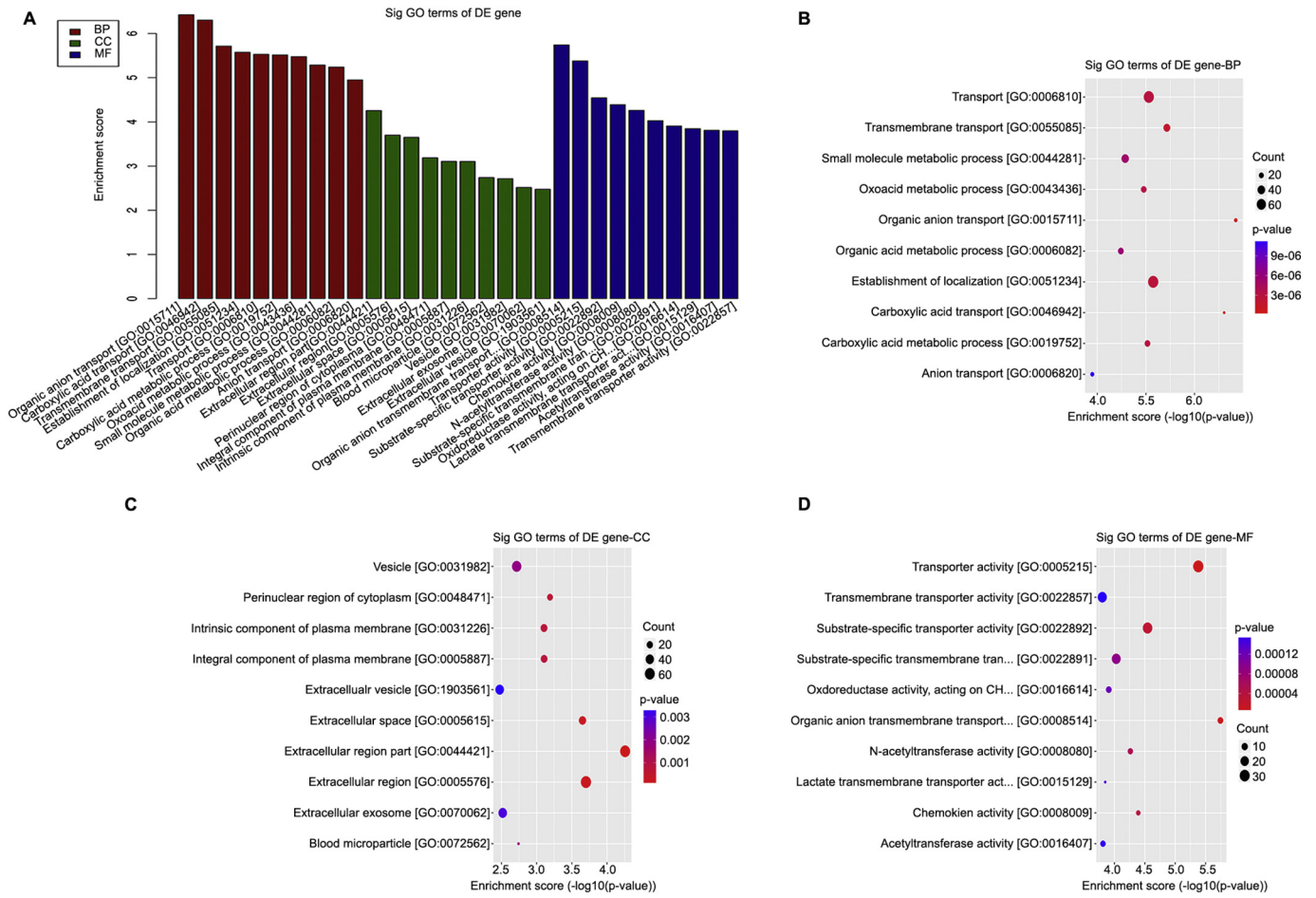

Fig. 6. GO analysis of up-regulated differentially expressed genes. (A) The top 10 most significantly enriched GO terms in three ontologies including biological process (BP), cellular component (CC), and molecular function (MF) are shown. The *P* values are arranged from lowest to highest along the X-axis. (B–D) Details regarding the number of up-regulated differentially expressed genes related to biological process (B), cellular component (C), and molecular functions (D) are summarized.

reactions were performed in an ABI 7500 system (ABI, USA) using SYBR Green Supermix (TaKaRa, Japan) according to the manufacturer's instructions. For each gene, reactions were performed using three RNA samples, and each reaction was performed in triplicate. The relative expression of differentially expressed genes was calculated according to the $2^{-\Delta\Delta Ct}$ method [35] using GAPDH for normalization. Continuous data are presented as means ± standard deviation (SD), and were analyzed by using one-way ANOVA, with the Tukey's post hoc test. Statistical analysis was performed in the SPSS version 16.0 software (SPSS, USA). A P value < 0.05 was considered significant.

3. Results

3.1. Establishment of rat DN STZ model and treatment with Art

The DN model was created in rats by intraperitoneal inject with STZ followed by treatment with Art. Masson and H&E staining showed increased glomerular hypertrophy and glomerular capillary dilatation in the STZ group compared with the normal control, and PAS staining showed increased glomerular hypertrophy and hyperplasia of glomeruli (Fig. 1A). The relative kidney weight in and the area and diameters of glomeruli in STZ and Art groups were significantly increased compared to those in normal group, indicating renal changes and glomerular hypertrophy ($P < 0.05$), while those were statistically reduced in Art group compared to STZ group ($P < 0.05$) (Fig. 1B–C). Moreover, the levels of FBG, urine protein, BUN, Cr, LDL-C, TG, and TC were significantly increased after the treatment with STZ, while insulin level decreased compared with control rats, providing further evidence of successful construction of the DN model (Fig. 2). However, Art inhibited glomerular hypertrophy, glomerular capillary dilatation, and hyperplasia of glomeruli. Art also reversed the effect of STZ by down-regulating FBG, urine protein, BUN, Cr, LDL-C, TG, and TC and elevating insulin level (Fig. 2). Thus to some degree, treatment with Art alleviated the STZ-induced DN.

3.2. Overview of gene expression prolife

In order to profile global gene expression in the samples, RNA-seq was determined using Illumina HiSeq 4000. A total of 13,292 genes and 16,056 transcripts in the normal control group, 13,243 genes and 15,978 transcripts in the STZ group, and 13,248 genes and 16,038 transcripts in the Art group were identified. Unsupervised hierarchical clustering of gene expression patterns clearly separated the Art and STZ groups (Fig. 3A). The scatter plot of the gene expression profile was used to assess the variations between Art and STZ groups (Fig. 3B). Differentially expressed genes with statistical significance between the Art and STZ groups were identified using a volcano plot (Fig. 3C). Overall, 462 genes were discovered to be significantly differentially expressed between Art and STZ groups (i.e., > 2-fold change and $P < 0.05$). Among them, 231 genes were significantly up-regulated and 231 genes were significantly down-regulated in Art samples, compared to STZ samples. A total of 31 genes significantly were up-

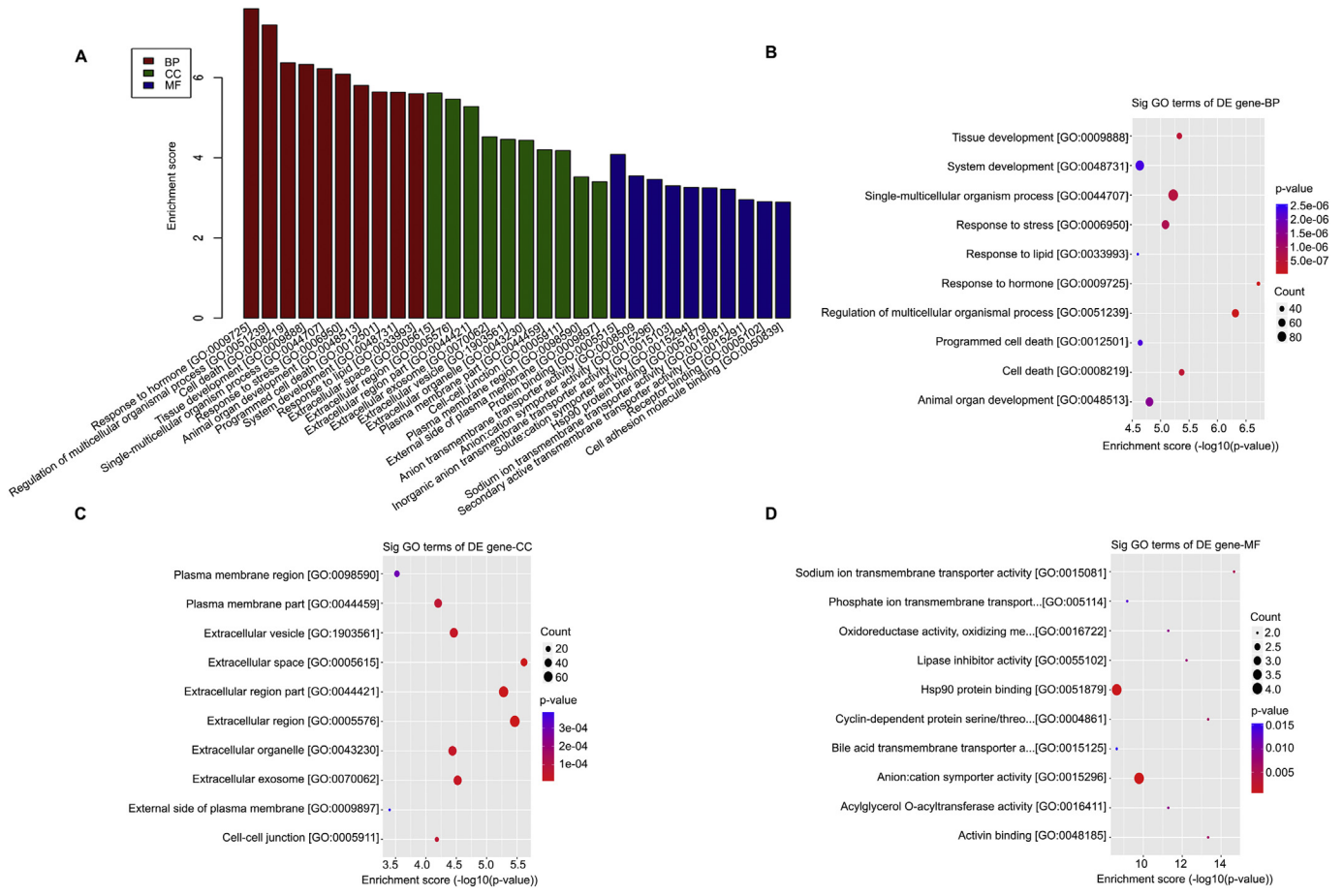

Fig. 7. GO-enriched items of down-regulated differentially expressed genes. (A) The top 10 most significantly enriched GO terms in biological process (BP), cellular component (CC), and molecular function (MF). The *P* values are arranged from low to high along the X-axis. (B–D) Details regarding the number of down-regulated differentially expressed genes associated with biological process (B), cellular component (C), and molecular functions (D) are summarized.

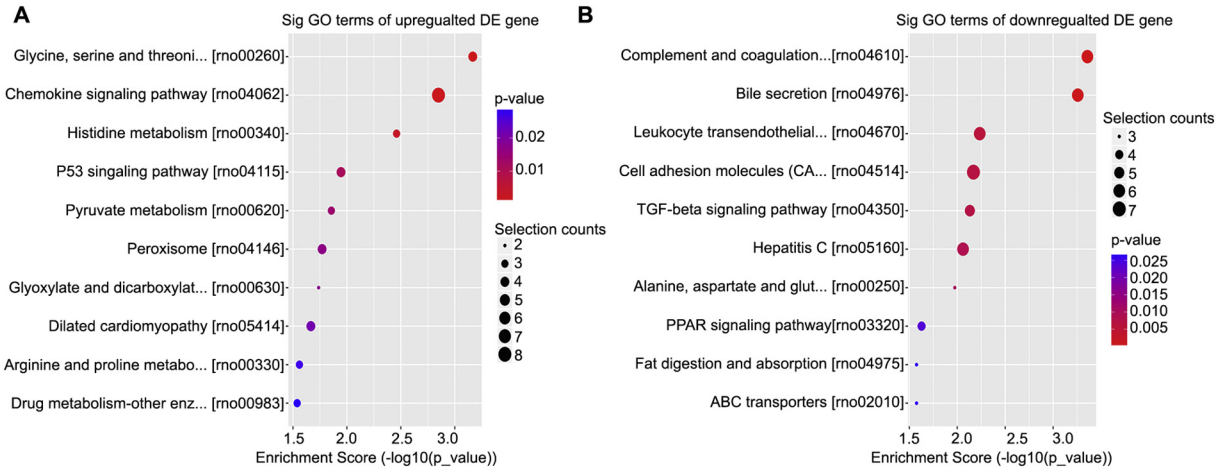

Fig. 8. Enriched KEGG pathway of differentially expressed genes. (A) KEGG pathways of up-regulated genes. (B) KEGG pathways of down-regulated genes. The top 10 most significantly enriched pathways were shown. Details regarding the number of differentially expressed genes related to KEGG pathway are also shown.

regulated in STZ samples compared to either normal samples or Art samples, and 38 genes were significantly down-regulated in STZ samples compared to either normal samples or Art samples (Tables 1 and 2). Unsupervised hierarchical clustering of the 70 common differentially expressed genes between STZ/normal and STZ/Art groups clearly separated the normal, Art, and STZ groups (Fig. 4), demonstrating that the identified differentially expressed genes are significant indicators for STZ treatment.

3.3. Verification of differentially expressed genes

Eight differentially expressed genes were randomly selected including four up-regulated genes *Id1* previously described to inhibit USF2 and block TGF-beta-induced apoptosis in mesangial cells (Sato et al.), *Cdkn1a*, *Hmgcs2* and *Rarres2* and four down-regulated genes *Igfbp1*, *Sult1a1*, *Pigr* and *Steap4* for further validation by using qRT-PCR (Fig. 5). Data on the expressions of these genes were totally consistent

with the findings from RNA-Seq.

3.4. GO analysis of differentially expressed genes

To explore the functions of differentially expressed genes, GO analysis was performed (Figs. 6 and 7). For up-regulated differentially expressed genes, we found that the most significant enriched GO term in the biological process was organic anion transport [GO:0015711] (Fig. 6A and B), the most significant enriched GO term in cellular component was extracellular region part [GO:0044421] (Fig. 6A and C), and the most significant enriched GO term in molecular function was organic anion transmembrane transporter activity [GO:000008541] (Fig. 6A and D).

For down-regulated differentially expressed genes, we found that the most significant enriched GO term in the biological process was response to hormone [GO:0009725] (Fig. 7A and B), the most significant enriched GO term in cellular component was extracellular space [GO:0005615] (Fig. 7A and C), and the most significant enriched GO term in molecular function was protein binding [GO:0005515] (Fig. 7A and D).

3.5. KEGG pathways of differentially expressed genes

The KEGG pathway of differentially expressed genes was also used (Fig. 8) and indicated that 10 most enriched pathways for up-regulated and down-regulated genes might be involved in DN (Fig. 8). Among these pathways, the up-regulated genes showed a strong relationship with the gene category “Glycine, serine and threonine metabolism [rno:00260]” (Fig. 8A), and the down-regulated genes showed a strong relationship with “Complement and coagulation cascades [rno:04610]” (Fig. 8B).

4. Discussion

Previous studies have reported a renoprotective role of Art in diabetic rats [19–24]. In those studies, Art was shown to alleviate pathological renal changes in diabetic rats, but the underlying molecular mechanisms were not fully understood. Early high-throughput studies of DN have been reported in the literature [25,27,36]. However, sequencing results for DN after Art treatment have not been reported previously. The present study was the first to investigate the gene expression prolife in DN rats treated with Art using RNA-Seq and provided useful information for understanding the molecular mechanism underlying treatment of DN by Art.

First, we constructed a rat DN model. STZ has been widely used in the construction of rat DN models [37–39]. The rats were then treated with Art. The resulting pathological changes such as increased glomerular hypertrophy and hyperplasia of glomeruli, along with increased FBG, urine protein, BUN, Cr, LDL-C, TG, TC, as well as decreased insulin level, provided evidence of successful construction of the DN model [29,40]. After treatment with Art, all of the injuries were ameliorated, confirming the renoprotective role of Art in diabetic rats. Then, samples were collected and RNA-Seq was performed.

By analyzing and validating the results of RNA-Seq, we identified a total of 13,292 genes and 16,056 transcripts in normal samples, 13,243 genes and 15,978 transcripts in STZ samples, and 13,248 genes and 16,038 transcripts in Art samples. We found that the gene expression levels were different among the normal samples, STZ samples, and Art treatment samples. In total, 31 genes, including solute carrier organic anion transporter family member 1A1 (*Slco1a1*), cytochrome P450 2C11 (*Cyp2c11*), prostaglandin-H2 D-isomerase (*Ptgds*), solute carrier family 16 member 14 (*Slc16a14*), 3-hydroxy-3-methylglutaryl-CoA synthase 2 (*Hmgcs2*), and inhibitor of DNA binding 1 (*Id1*), were significantly up-regulated in STZ samples compared to both normal and Art samples, and 38 genes, including insulin like growth factor binding protein 1 (*Igfbp1*), follistatin (*Fst*), fin bud initiation factor homolog (*Fibin*), sulfotransferase 1A1 (*Sult1a1*), and beta-defensin (*Defb28*) were significantly down-regulated in STZ samples compared to both normal and Art samples, with changes > 2-fold, and *P*-value < 0.05. A previous study also reported reductions in levels of *Ptgds* and *Id1*. Moreover, we randomly selected four up-regulated genes (including *Id1, Cdkn1a, Hmgcs2,* and *Rarres2*) and one down-regulated gene (*IGFBP1, Sult1a1, Pigr, Steap4*) to evaluate expression levels using qRT-PCR in all of the normal, STZ, and Art samples. Our results showed consistency in qRT-PCR and RNA-Seq data. It was demonstrated that ID1 is a risk factor for obesity and diabetes. In the late phase of diabetic glomerulopathy, ID1 inhibits TGF-β-induced apoptosis in mesangial cells [41]. The overexpression of CDKN1A in pancreatic islet B cells results in impaired insulin secretion and a decrease in islet B cell proliferation [42]. Diabetic kidneys exhibit excess ketogenic activity resulting from increased HMGCS2 expression, which may also be involved in the pathogenesis of DN [43]. Thus, our data on up-or down-expression of those genes in DN were consistent with previous studies and indicated that the RNA-Seq data were reliable.

Moreover, the top 10 known pathways and biological processes associated with the up-regulated and down-regulated genes were included. For instance, GO analysis and pathway analysis were carried out to explore the potential biological functions and mechanisms of differentially expressed genes in the treatment of DN by Art. Specifically, the potential biological processes were organic anion transport, carboxylic acid transport, and response to hormone. The potential cellular components were extracellular region part, and extracellular space. Predicted molecular functions were organic anion transmembrane transporter activity, protein binding. Among the GO terms associated with differentially expressed genes, response to hormone has been reported to be involved in the treatment of DN [44,45]. Pathways involving “Glycine, serine and threonine metabolism”, “Complement and coagulation cascades”, “p53 signaling pathway”, “TGF-beta signaling pathway”, and “PPAR signaling pathway” were also included. Among the KEGG pathways, complement and coagulation cascades have been reported to play an important role in the progression of DN [46]. It has also been reported that the p53, TGF-beta signaling pathways are associated with DN [47,48]. Imbalanced expression of certain genes is believed to cause aberrant cellular functions in the kidney. Our preliminary study provided leads on the potential roles of genes in the pathogenesis of DN. For instance, our data suggested possible alterations in the level of glutathione-S-transferase, which was consistent with previous transcriptomic analysis of DN in STZ-induced diabetic rats [49]. Functional genomics studies will further clarify the effect of genes in DN. Additionally, these results will likely provide more focused scientific guidance for investigating the effects of Art in DN. Art was able to convert glucagon-producing alpha cells into insulin-producing beta cells. So we also evaluated the level of insulin among three groups. Our result showed insulin level was decreased compared with control rats after the treatment with STZ, providing further evidence of successful construction of the DN model. By contrast, Art reversed the effect of STZ by down-regulating FBG, urine protein, BUN, Cr, LDL-C, TG, and TC and elevating insulin level. Concordantly, data from both RNA-seq and qPCR indicated that insulin-like growth factor binding protein 1 gene (*Igfbp1*) was also elevated after administration of Art in STZ-treated model, indicating Art plays a promoting role in the restoration of blood insulin levels. However, the limitation still exists that the differentially expressed genes obtained in the transcriptome analysis, except eight genes involved in this study, require further validation by RT-qPCR, which may provide fundamental leads for the development of anti-DN therapy.

5. Conclusion

In conclusion, we have successfully constructed a differentially gene expression profile of DN in a rat model. Using bioinformatic analysis, we provided a detailed analysis of the molecular mechanisms and

effects of Art in DN.

Supplementary data to this article can be found online at https://doi.org/10.1016/j.lfs.2019.01.032.

Data availability statements

The data generated to support the findings of this study are included within the article.

Conflict of interest

All authors declare no potential conflict of interest.

Acknowledgements

This work was supported by Shenzhen Science and Technology Project (Grant No. JCYJ20140408152909279).

Author contributions

Contributed to the conception and design of the experiment: MX, JDL; Performed the experiments: MX, LPH; Analyzed the data: ZHC, GLX; Wrote the manuscript: JDL. All authors approved revisions and the final paper.

References

[1] S.N. Uwaezuoke, The role of novel biomarkers in predicting diabetic nephropathy: a review, Int. J. Nephrol. Renov. Dis. 10 (2017) 221–231.
[2] T. Wu, S. Qiao, C. Shi, S. Wang, G. Ji, The metabolomics window into diabetic complications, J. Diabetes Investig. 9 (2017) 244–255.
[3] U.A.A. Sharaf El Din, M.M. Salem, D.O. Abdulazim, Diabetic nephropathy: time to withhold development and progression - a review, J. Adv. Res. 8 (2017) 363–373.
[4] K. Tanabe, Y. Maeshima, Y. Sato, J. Wada, Antiangiogenic therapy for diabetic nephropathy, Biomed. Res. Int. 2017 (2017) 5724069.
[5] G.H. Tesch, Diabetic nephropathy - is this an immune disorder? Clin. Sci. (Lond.) 131 (2017) 2183–2199.
[6] H. Dai, Q. Liu, B. Liu, Research Progress on mechanism of podocyte depletion in diabetic nephropathy, J. Diabetes Res. 2017 (2017) 2615286.
[7] M. Kitada, Y. Ogura, I. Monno, D. Koya, Regulating autophagy as a therapeutic target for diabetic nephropathy, Curr. Diab. Rep. 17 (2017) 53.
[8] J. Egido, J. Rojas-Rivera, S. Mas, M. Ruiz-Ortega, A.B. Sanz, E. Gonzalez Parra, et al., Atrasentan for the treatment of diabetic nephropathy, Expert Opin. Investig. Drugs 26 (2017) 741–750.
[9] L. Cui, X.Z. Su, Discovery, mechanisms of action and combination therapy of artemisinin, Expert Rev. Anti-Infect. Ther. 7 (2009) 999–1013.
[10] P. Olliaro, Mode of action and mechanisms of resistance for antimalarial drugs, Pharmacol. Ther. 89 (2001) 207–219.
[11] J. Wang, J. Zhang, Y. Shi, C. Xu, C. Zhang, Y.K. Wong, et al., Mechanistic investigation of the specific anticancer property of artemisinin and its combination with aminolevulinic acid for enhanced anticolorectal cancer activity, ACS Cent. Sci. 3 (2017) 743–750.
[12] T. Wei, J. Liu, Anti-angiogenic properties of artemisinin derivatives (review), Int. J. Mol. Med. 40 (2017) 972–978.
[13] L. Hou, H. Huang, Immune suppressive properties of artemisinin family drugs, Pharmacol. Ther. 166 (2016) 123–127.
[14] Z.M. Lin, X.Q. Yang, F.H. Zhu, S.J. He, W. Tang, J.P. Zuo, Artemisinin analogue SM934 attenuate collagen-induced arthritis by suppressing T follicular helper cells and T helper 17 cells, Sci. Rep. 6 (2016) 38115.
[15] J. Cao, W. Wang, Y. Li, J. Xia, Y. Peng, Y. Zhang, et al., Artesunate attenuates unilateral ureteral obstruction-induced renal fibrosis by regulating the expressions of bone morphogenetic protein-7 and uterine sensitization-associated gene-1 in rats, Int. Urol. Nephrol. 48 (2016) 619–629.
[16] P. Lu, F.C. Zhang, S.W. Qian, X. Li, Z.M. Cui, Y.J. Dang, et al., Artemisinin derivatives prevent obesity by inducing browning of WAT and enhancing BAT function, Cell Res. 26 (2016) 1169–1172.
[17] W.E. Ho, H.Y. Peh, T.K. Chan, W.S. Wong, Artemisinins: pharmacological actions beyond anti-malarial, Pharmacol. Ther. 142 (2014) 126–139.
[18] J. Li, T. Casteels, T. Frogne, C. Ingvorsen, C. Honore, M. Courtney, et al., Artemisinins target GABAA receptor signaling and impair alpha cell identity, Cell 168 (2017) 86–100.e15.
[19] L. Zhang, Y. Su, F. Zhou, J. Zhang, Z. An, Effect of Artemisinin on the upregulation of PDGF-B protein expression in the kidney of experimental diabetic rats, Mod. J. Integr. Tradit. Chin. West. Med. 23 (2014) 1392–1393.
[20] L. Zhang, J. Zhang, F. Zhou, Y. Su, Z. An, Inhibitory effect of artemisinin on the spatiotemporal dynamics activation of protein kinase C in the kidney of experimental diabetic rats, Mod. J. Integr. Tradit. Chin. West. Med. 18 (2014) 1964–1966.
[21] L. Zhang, F. Zhou, Y. Su, J. Zhang, Z. An, Study on the mechanism of renoprotective effects of artemisinin in diabetic rats, Mod. J. Integr. Tradit. Chin. West. Med. 26 (2014) 2862–2864.
[22] F. Zhou, Y. Su, L. Zhang, J. Zhang, Z. An, Inhibitory effect of artemisinin on the upregulation of DNA-binding activity of NF-κB in kidney tissue of diabetic rats, Mod. J. Integr. Tradit. Chin. West. Med. 15 (2014) 2075–2079.
[23] F. Zhou, J. Zhang, L. Zhang, Y. Su, Z. An, Inhibitory effect of artemisinin on the upregulation of the DNA-binding activity of AP-1 in the kidney tissue of experimental diabetic rats, Mod. J. Integr. Tradit. Chin. West. Med. 24 (2014) 2648–2649.
[24] F. Zhou, L. Zhang, Y. Su, J. Zhang, Z. An, Inhibitory effect of artemisinin on the upregulation of c-fos and c-jun gene expression in kidney tissue of diabetic rats, Mod. J. Integr. Tradit. Chin. West. Med. 21 (2014) 2294–2295.
[25] M. Rudnicki, A. Beckers, H. Neuwirt, J. Vandesompele, RNA expression signatures and posttranscriptional regulation in diabetic nephropathy, Nephrol. Dial. Transplant. 30 (Suppl. 4) (2015) iv35–42.
[26] E.P. Brennan, M.J. Morine, D.W. Walsh, S.A. Roxburgh, M.T. Lindenmeyer, D.P. Brazil, et al., Next-generation sequencing identifies TGF-beta1-associated gene expression profiles in renal epithelial cells reiterated in human diabetic nephropathy, Biochim. Biophys. Acta 1822 (2012) 589–599.
[27] K.J. Kelly, Y. Liu, J. Zhang, C. Goswami, H. Lin, J.H. Dominguez, Comprehensive genomic profiling in diabetic nephropathy reveals the predominance of proinflammatory pathways, Physiol. Genomics 45 (2013) 710–719.
[28] G. Xu, Y.L. Huang, P.L. Li, H.M. Guo, X.P. Han, Neuroprotective effects of artemisinin against isoflurane-induced cognitive impairments and neuronal cell death involve JNK/ERK1/2 signalling and improved hippocampal histone acetylation in neonatal rats, J. Pharm. Pharmacol. 69 (2017) 684–697.
[29] Y.D. Jeon, S.H. Kang, K.H. Moon, J.H. Lee, D.G. Kim, W. Kim, et al., The effect of *Aronia* berry on type 1 diabetes in vivo and in vitro, J. Med. Food 21 (2018) 244–253.
[30] K. Mise, T. Ueno, J. Hoshino, R. Hazue, K. Sumida, M. Yamanouchi, et al., Nodular lesions in diabetic nephropathy: collagen staining and renal prognosis, Diabetes Res. Clin. Pract. 127 (2017) 187–197.
[31] A. Shah, L. Xia, E.A. Masson, C. Gui, A. Momen, E.A. Shikatani, et al., Thioredoxin-interacting protein deficiency protects against diabetic nephropathy, J. Am. Soc. Nephrol. 26 (2015) 2963–2977.
[32] Y.L.Y. Qian, C. Rui, Y. Qian, M. Cai, R. Jia, Potential significance of circular RNA in human placental tissue for patients with preeclampsia, Cell. Physiol. Biochem. 39 (2016) 1380–1390.
[33] N. Whiteford, T. Skelly, C. Curtis, M.E. Ritchie, A. Lohr, A.W. Zaranek, et al., Swift: primary data analysis for the Illumina Solexa sequencing platform, Bioinformatics 25 (2009) 2194–2199.
[34] Y. Zeng, J.X. Liu, Z.P. Yan, X.H. Yao, X.H. Liu, Potential microRNA biomarkers for acute ischemic stroke, Int. J. Mol. Med. 36 (2015) 1639–1647.
[35] J.X. Liu, Z.P. Yan, Y.Y. Zhang, J. Wu, X.H. Liu, Y. Zeng, Hemodynamic shear stress regulates the transcriptional expression of heparan sulfate proteoglycans in human umbilical vein endothelial cell, Cell Mol. Biol. (Noisy-le-grand) 62 (2016) 28–34.
[36] A.L. Mooyaart, Genetic associations in diabetic nephropathy, Clin. Exp. Nephrol. 18 (2014) 197–200.
[37] L. An, M. Zhou, F. Marikar, X.W. Hu, Q.Y. Miao, P. Li, et al., Salvia miltiorrhiza lipophilic fraction attenuates oxidative stress in diabetic nephropathy through activation of nuclear factor erythroid 2-related factor 2, Am. J. Chin. Med. (2017) 1–17.
[38] S. Yang, J. Zhang, S. Wang, J. Shi, X. Zhao, Knockdown of angiopoietin-like protein 2 ameliorates diabetic nephropathy by inhibiting TLR4, Cell. Physiol. Biochem. 43 (2017) 685–696.
[39] Y.W. Zhang, X. Wang, X. Ren, M. Zhang, Involvement of glucose-regulated protein 78 and spliced X-box binding protein 1 in the protective effect of gliclazide in diabetic nephropathy, Diabetes Res. Clin. Pract. 146 (2017) 41–47.
[40] Q.Y. Wang, F.Q. Chen, Clinical significance and different levels of urinary monocyte chemoattractant protein-1 in type 2 diabetes mellitus, Diabetes Res. Clin. Pract. 83 (2009) 215–219.
[41] A.Y. Sato, E. Antonioli, R. Tambellini, A.H. Campos, ID1 inhibits USF2 and blocks TGF-beta-induced apoptosis in mesangial cells, Am. J. Physiol. Ren. Physiol. 301 (2011) F1260–F1269.
[42] A.M. Hernandez, E.S. Colvin, Y.C. Chen, S.L. Geiss, L.E. Eller, P.T. Fueger, Upregulation of p21 activates the intrinsic apoptotic pathway in beta-cells, Am. J. Physiol. Endocrinol. Metab. 304 (2013) E1281–E1290.
[43] D. Zhang, H. Yang, X. Kong, K. Wang, X. Mao, X. Yan, et al., Proteomics analysis reveals diabetic kidney as a ketogenic organ in type 2 diabetes, Am. J. Physiol. Endocrinol. Metab. 300 (2011) E287–E295.
[44] D. Mukhi, R. Nishad, R.K. Menon, A.K. Pasupulati, Novel actions of growth hormone in podocytes: implications for diabetic nephropathy, Front. Med. (Lausanne) 4 (2017) 102.
[45] S. Shelbaya, M.M. Abushady, M.S. Nasr, M.M. Bekhet, Y.A. Mageed, M. Abbas, Study of irisin hormone level in type 2 diabetic patients and patients with diabetic nephropathy, Curr. Diabetes Rev. 14 (2017) 481–486.
[46] Z. Wang, Z. Wang, Z. Zhou, Y. Ren, Crucial genes associated with diabetic nephropathy explored by microarray analysis, BMC Nephrol. 17 (2016) 128.
[47] J. Sheng, H. Li, Q. Dai, C. Lu, M. Xu, J. Zhang, et al., NR4A1 promotes diabetic nephropathy by activating Mff-mediated mitochondrial fission and suppressing Parkin-mediated mitophagy, Cell. Physiol. Biochem. 48 (2018) 1675–1693.
[48] W.N. Wang, W.L. Zhang, G.Y. Zhou, F.Z. Ma, T. Sun, S.S. Su, et al., Prediction of the molecular mechanisms and potential therapeutic targets for diabetic nephropathy by bioinformatics methods, Int. J. Mol. Med. 37 (2016) 1181–1188.
[49] C. Lomas-Soria, M. Ramos-Gomez, L. Guevara-Olvera, R. Guevara-Gonzalez, I. Torres-Pacheco, M.A. Gallegos-Corona, et al., Transcriptomic analysis in diabetic nephropathy of streptozotocin-induced diabetic rats, Int. J. Mol. Sci. 12 (2011) 8431–8448.